Depolymerizable and recyclable luminescent polymers with high light-emitting efficiencies

Wei Liu [1,8], Yukun Wu [2,3,8], Aikaterini Vriza[2], Cheng Zhang [1], Hyocheol Jung [2,7], Shiyu Hu [4], Yuepeng Zhang [4], Du Chen [5,6], Peijun Guo [5,6], Benjamin T. Diroll[2], Glingna Wang [1], Richard D. Schaller [2], Henry Chan [2], Jianguo Mei [3] ✉, Sihong Wang [1,2] ✉ & Jie Xu [1,2] ✉

Luminescent polymers are of great interest in a number of photonic technologies, including electroluminescence, bioimaging, medical diagnosis, bio-stimulation and security signage. Incorporating depolymerizability and recyclability into luminescent polymers is pivotal for promoting their sustainability and minimizing their environmental impacts at the end of the product lifecycle, but existing strategies often compromise the light-emitting efficiencies. Here we develop a strategy that utilizes cleavable moiety to create depolymerizable and recyclable thermally activated delayed fluorescence (TADF) polymers without compromising their high light-emitting efficiencies. The electroluminescent devices based on the TADF polymers achieved a high external quantum efficiency of up to 15.1%. The TADF polymers can be depolymerized under either mild acidic or heating conditions, with precise control of the kinetics, and the obtained pure monomers can potentially be isolated and repolymerized for subsequent life applications. This work promotes the end-of-life environmental friendliness and circularity of luminescent materials, paving the way to a sustainable photonic industry.

Organic luminescent materials have been widely used as the key materials in a number of photonic technologies, including electroluminescence (EL)[1], fluorescent bioimaging[2] and optical therapies[3]. Taking EL application as an example, with the advent of modern display development, emerging trends such as large-area, foldable and stretchable displays, as well as low-cost manufacturing, have led to rapid development and applications of luminescent materials including polymeric systems[1,4,5]. This is due to their solution processability, mechanical deformability and chemical tunability. Accompanied by the rapidly increased use of luminescent polymers, on the other hand, the end-life disposal of these polymers, similar to the plastic pollution issues of commodity polymers[6,7], could potentially pose severe threats to the environment[8,9]. Therefore, it is essential to incorporate degradability (that is, depolymerizability) into polymer-type luminescent materials to minimize their impact on the environment[6,9–18]. Despite efforts to endow degradable properties to a polymer, that is, poly(lactic acid) with
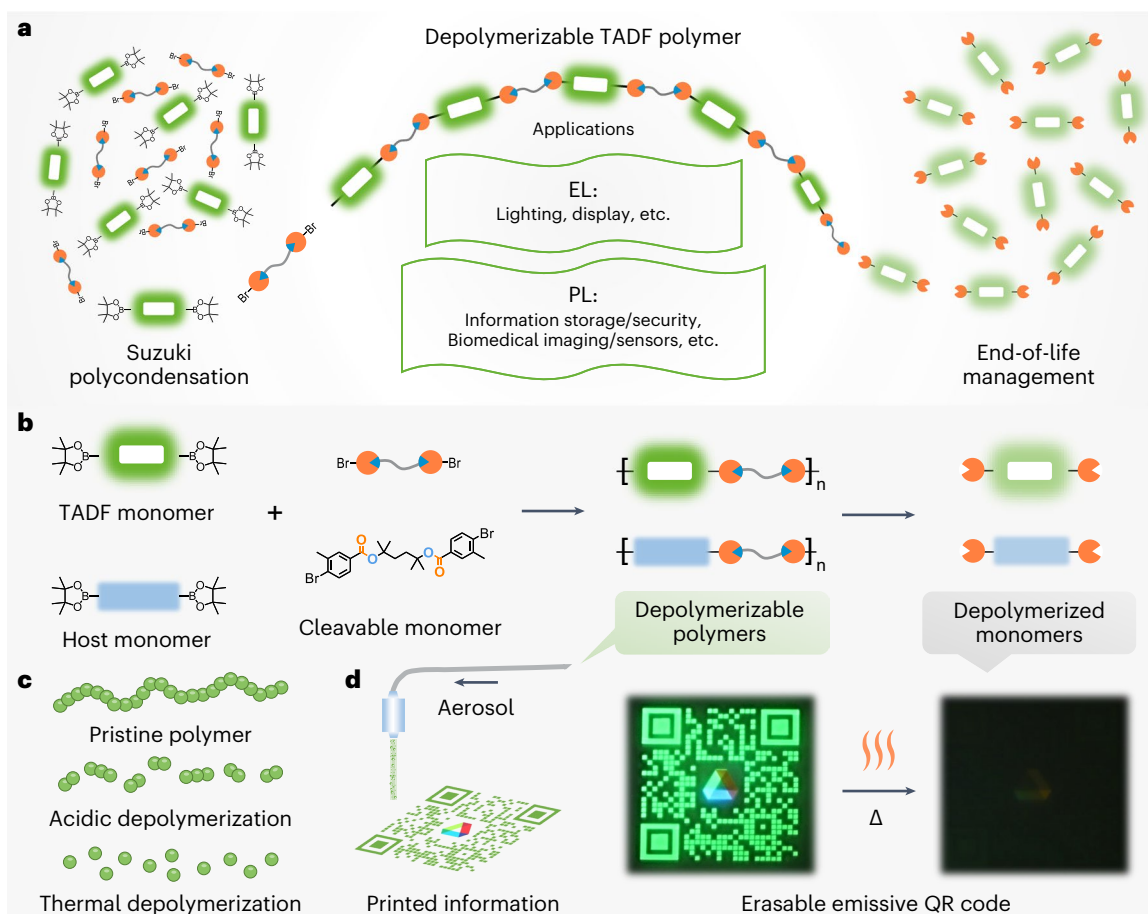
Fig. 1 | Depolymerizable luminescent polymers based on TADF mechanism and cleavable chemistry. a, Design principle for realizing depolymerizable TADF polymers via incorporation of TB-ester cleavable bond into the polymer backbone. The lifetime of depolymerizable TADF polymers from synthesis via Suzuki polycondensation towards various potential applications and the end-of-life management by depolymerization to pure monomers. **b**, Schematic of incorporating TB-ester cleavable bond into two types of functional materials, polymeric TADF emitter and polymeric TADF host used in the EML of EL devices, as well as the depolymerization mechanisms. **c**, Schematic of pristine polymer, oligomer-product by the acidic depolymerization, and pure monomer-product by the thermal depolymerization. **d**, Prototype application for the depolymerizable polymers for information storage/security. The glass sheet with the printed QR code is placed on a heat plate at 210 °C in N_2 atmosphere for 1 h to erase the pattern. The pictures are captured at room temperature. A timeline of images is provided in Supplementary Fig. 20. A Thorlabs CS20 UV LED System (365 nm) is used for the photoexcitation.

a fluorescent tag, only low external quantum efficiencies (EQE) in EL devices (not more than 1.5%) have been achieved[19]. This polymer design is based on fluorescence (FL) type emitters, and their efficiency is fundamentally limited by their photophysical nature. Organic light-emitting diodes (OLED) utilizing fluorescent emitters, which are excited by electron–hole recombination, only harvest the singlet excitons for emission allowing for an internal quantum efficiency of 25% at best.

To maintain the relevance to practical technologies, depolymerizable luminescent polymers need to have high light-emitting efficiencies, which, in the case of electro-excitation, can be achieved by either spin–orbit coupling-induced phosphorescence (PH)[20] or thermally activated delayed fluorescence (TADF)[21,22]. Among these two options, TADF emitters have attracted increasing interest in polymer designs due to potentially lower costs and transition metal-free designs. By minimizing the singlet and triplet energy states splitting (ΔE_{ST}), TADF emitters can convert non-radiative triplet excitons into radiative singlet excitons through reverse intersystem crossing (RISC), offering a pathway towards 100% internal quantum efficiencies[21]. However, to the best of our knowledge, there has been no report on imparting depolymerizability/recyclability into a TADF polymer. There are several challenges associated with this, including (1) selecting cleavable linkages that are compatible with the TADF emission (especially not quenching long-lived triplet excitons), while not preventing efficient

charge transport; (2) designing and synthesizing TADF polymers with those cleavable linkage points; (3) controllable depolymerization features—dormant in the operational environment but responsive to external stressors after the service life.

In this Article, we develop a general design concept that utilizes cleavable moiety to create depolymerizable luminescent polymers with high EL performance enabled by TADF, and programmable depolymerizations under specific stressors (Fig. 1a). Our design employs *tert*-butyl ester (TB-ester), which we experimentally confirmed to be benign to TADF properties. We successfully applied this concept to a TADF polymer, as well as a host polymer for small-molecule TADF guests. A combination of the host polymer and TADF guest achieved an EQE of up to 15.1%, which is an order of magnitude higher than the previously reported system that utilized a depolymerizable luminescent guest polymer[19]. These polymers can be depolymerized under either mild acidic or heating conditions, with precise control of the kinetics for the final products of either oligomers or pure monomers and within a range of time windows from several days down to minutes (Fig. 1b,c). Furthermore, the pure monomers produced from thermal depolymerization can potentially be isolated and repolymerized for subsequent life applications. We expect that our polymers not only can be used for existing (photoluminescence) PL and EL technologies such as displays, medical imaging, optical stimulation, but also enable new applications
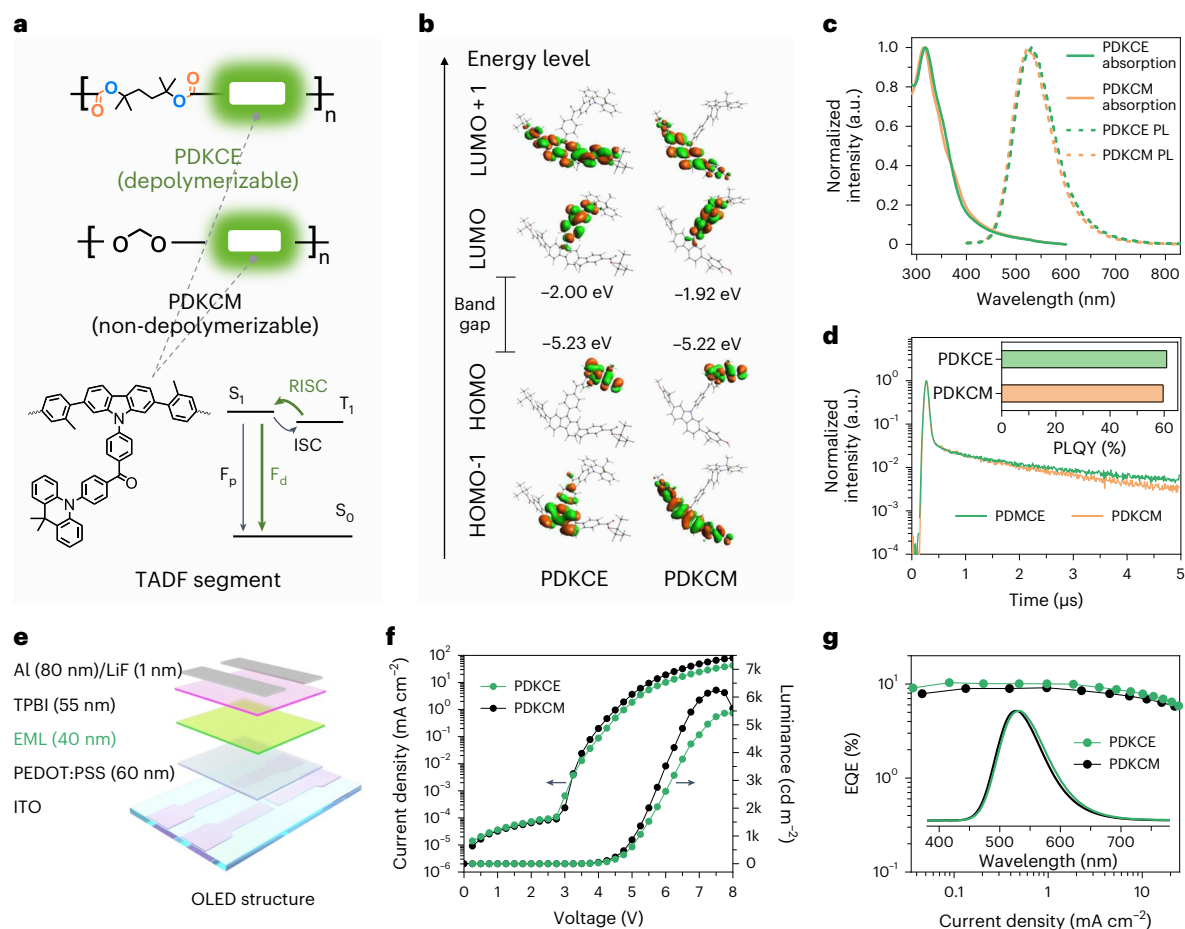
Fig. 2 | PL and EL properties of the depolymerizable TADF polymer PDKCE.
a, The chemical structures of depolymerizable TADF polymer PDKCE and
its control polymer PDKCM, and the mechanism of TADF. S_0, S_1 and T_1 stand
for ground state, lowest singlet state and lowest triplet state energy levels,
respectively. ISC and RISC, respectively stand for intersystem crossing and
reverse ISC. F_p and F_d stand for prompt fluorescence and delayed fluorescence,
respectively. **b**, DFT-calculated HOMO, LUMO, HOMO-1 and LUMO + 1 distributions,
as well as energy levels in the smallest electronic conjugation units of PDKCE
and PDKCM. **c**, The absorption spectra, and room temperature emission
spectra from the thin films of PDKCE and PDKCM. The emission spectra are
measured in air under excitation at 310 nm. **d**, PL transient decays and PLQYs
(insert) of PDKCE and PDKCM. **e**, Schematic structure of the OLED used in the
characterization of the EL performance of PDKCE and PDKCM as the host-free
EML. **f,g**, Representative current density–luminance–voltage traces (**f**) and EQE–
current density traces (**g**) as well as normalized EL spectra (inset in **g**) for PDKCE
and PDKCM.

such as printed erasable or hidden emissive quick-response (QR) codes
(Fig. 1d and Supplementary Video 1).

Results

Design of the depolymerizable TADF polymer
To introduce depolymerizability into TADF polymers, it is neces-
sary to incorporate a functional bond satisfying the following two
requirements. First, it remains stable throughout the device fabrica-
tion process and during the device working life without affecting the
TADF properties. Second, it can rapidly cleave under inflicted external
stressors. In this study, TB-ester was selected as the cleavable moiety,
whose scission can be triggered either by mild acidic conditions or
under elevated temperatures[23–25]. Additionally, the TB-ester exhibits
greater stability under base conditions compared with typical esters[24],
enabling its compatibility with a diverse range of reactions, including
the Suzuki polycondensation reaction. Moreover, it has been reported
in the literature that ester groups can be incorporated into TADF emit-
ters without negatively impacting the TADF properties[26,27].

In consideration of these aspects, we designed a depolymerizable
TADF polymer (namely PDKCE) with TB-ester moieties and TADF units
in the polymer backbone (Fig. 2a and Supplementary Figs. 1–3). The
TADF units were constructed by benzophenone and acridine as electron

acceptor (A) and donor (D) groups, respectively, which are attached as
pendant side groups to carbazole groups in the polymer backbone. To
investigate the impact of incorporating cleavable TB-ester bonds on
TADF properties, a control polymer PDKCM (Fig. 2a), studied in our pre-
vious work[4], with identical TADF units linked by non-depolymerizable
methylene diether groups is introduced for comparison. It is notewor-
thy that the synthesis of PDKCE follows a similar methodology as that
of PDKCM. While we utilized microwave-assisted synthesis techniques
to substantially reduce the polymerization time from several days to
less than 2 h, without any adverse impact on the molecular weight.

Photophysical and electroluminescence characterizations
To study the influences of TB-ester moiety on the TADF polymer's
luminescent property, density functional theory (DFT) based calcu-
lations were first performed to reveal the electronic structures. Since
TB-ester breaks the conjugation in the backbone, we performed the
DFT calculations on the repeating unit as it is reasonable to assume
that the photophysical properties and electronic structures of TADF
polymers will be largely determined by the smallest conjugation units
(Fig. 2b and Supplementary Fig. 4). Our calculations showed that in
PDKCE, the highest occupied molecular orbital (HOMO) and lowest
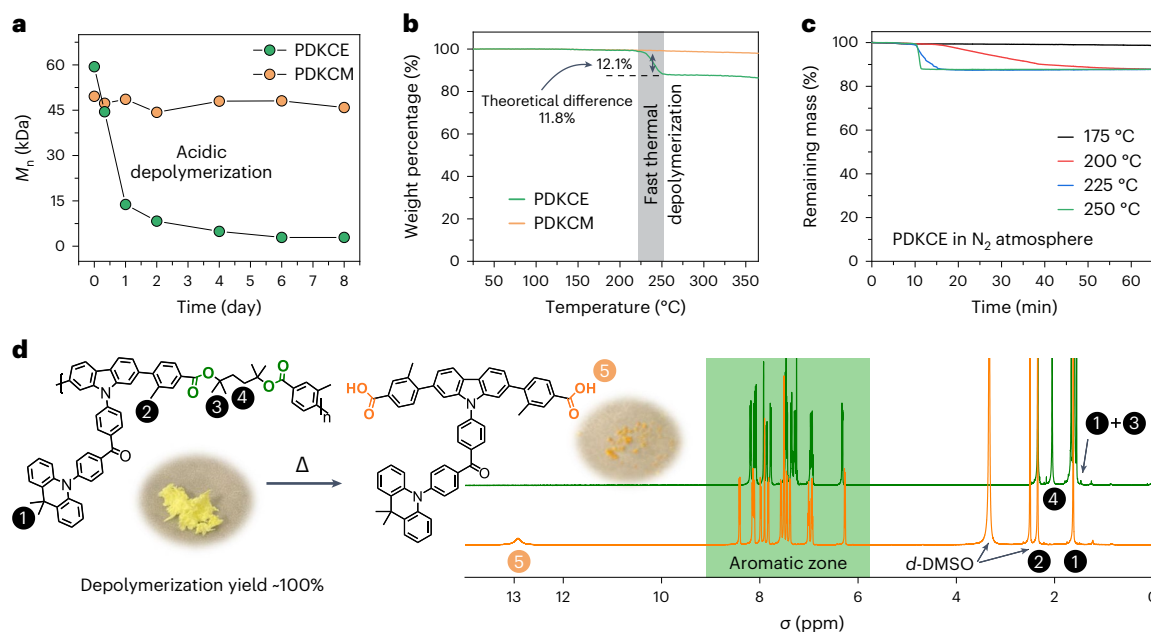unoccupied molecular orbital (LUMO) are respectively localized on the

Fig. 3 | The depolymerizability of PDKCE. a, The number average molar mass (M_n) of PDKCE and PDKCM monitored over time in the mixed THF/HCl solution. **b**, The TGA curves of PDKCE and PEKCM with a heating rate of 15 °C min⁻¹ in N₂ atmosphere. **c**, The TGA curves of PDKCE at different final temperatures, after initial heating at a rate of 15 °C min⁻¹ starting from 25 °C in N₂ atmosphere. **d**, The chemical structures, appearance and NMR spectra of PDKCE before and after thermal depolymerization.

D and A groups with minimum overlap, and the dihedral angle between the D and A planes remains orthogonal at 89.9° without much change resulting from the introduction of the TB-ester moieties (Fig. 2b). These results suggest that PDKCE possesses a small ΔE_{ST} (ref. 21), which is crucial for enabling the efficient RISC of excitons from the triplet state to the singlet state for TADF emission. As a comparison, similar results were observed in our control polymer PDKCM. However, in PDKCM, the HOMO-1 distribution extends from the carbazole group to the ether group, while in PDKCE, it is confined to the carbazole and part of the attached benzophenone groups. Conversely, the LUMO + 1 distribution stretched further away from the carbazole group onto the TB-ester groups in PDKCE. This notable difference can be attributed to the higher electron-deficient property of the TB-ester group compared with the ether group (Supplementary Fig. 5).

The impact of the TB-ester moieties on the PL properties was further investigated by conducting in-depth photophysical studies of PDKCE and the control polymer PDKCM. First, PDKCE and PDKCM give very similar ultraviolet–visible (UV–vis) absorption and PL spectra at room temperature (Fig. 2c), which agrees well both with the results of electrochemical cyclic voltammetry (CV) tests (Supplementary Fig. 6a) and DTF calculations discussed above. Estimated by the difference between the onset of low-temperature (77 K) FL/PH spectra (Supplementary Fig. 7), the ΔE_{ST} of PDKCE has a sufficiently small value of 59.0 meV, which is very close to that (46.9 meV) of PDKCM[4]. At room temperature, the PL quantum yield (PLQY) of PDKCE reaches 60.9%, which is composed of both prompt and delayed fluorescence as evidenced by the transient PL decay tests (Fig. 2d and Supplementary Fig. 8). Once again, these aspects are highly similar to those of PDKCM, indicating that the TB-ester bond has a limited impact on the overall TADF process.

Subsequently, we investigated the EL properties of the PDKCE in a conventional OLED structure (Fig. 2e and Supplementary Fig. 9). As a comparison, PDKCM was fabricated into the same device structure. As shown by the current density–voltage (J–V) and luminance–voltage (L–V) traces (Fig. 2f), PDKCE only exhibits a minor decrease in the current density and luminance compared to PDKCM. Since the HOMO/LUMO levels are similar for the two polymers, this small difference might be caused by the slightly decreased charge mobility, which was confirmed through the fabrication and measurement of hole-only devices (Supplementary Fig. 10). Additionally, we found a slight red shift in the EL spectrum for PDKCE, while little differences were observed for the turn-on voltages, efficiencies and device lifetimes (Fig. 2g and Supplementary Fig. 11). It is noteworthy that the achieved EQE of 10.4% from PDKCE is about seven times higher than previously reported depolymerizable luminescent polymer[19] (Supplementary Table 1).

Evaluation of the depolymerizability and recyclability

The depolymerizability of PDKCE is studied using two different stressors: acid and heat. It is found that the PDKCE chain can be effectively deconstructed by over 90% in a near-stomach acid condition[11] (that is, pH 1.2) within 4 days. This was evidenced by a decrease in the number average molar mass, as measured by size exclusion chromatography (SEC) (Fig. 3a and Supplementary Fig. 12). Such acidic degradation property affords the potential for the use in transient biomedical devices[14,28–30]. In comparison, the control polymer PDKCM shows no depolymerization under the same conditions (Fig. 3a). Furthermore, PDKCE has remarkable stability in harsh basic conditions (Supplementary Fig. 13), ensuring the compatibility with the synthesis conditions such as the utilized Suzuki polycondensation reaction.

Thermal stressor is also expected to degrade PDKCE by breaking the TB-ester bonds[23,24]. Thermal gravimetric analysis (TGA) shows that PDKCE remains stable up to 210 °C, after which a swift mass loss occurs between 210 and 250 °C, indicating depolymerization (Fig. 3b). The depolymerization rate of PDKCE can be finely controlled by selecting different depolymerization temperatures (Fig. 3c). The mass loss of 12.1% in TGA is almost equivalent to the theoretical weight value of 11.8% needed for PDKCE to generate the di-carboxylic acid group-capped monomers (Fig. 3b). Moreover, DFT calculations confirm that the TB-ester along the polymer backbone has a relatively weak bond energy by mapping the bond dissociation enthalpy[31] for the smallest conjugation units (Supplementary Fig. 14). Further analysis of the crude product of PDKCE from thermal depolymerization using nuclear magnetic resonance (NMR) and high-resolution mass spectroscopy (MS) shows that the depolymerization yields diacid monomers in very high
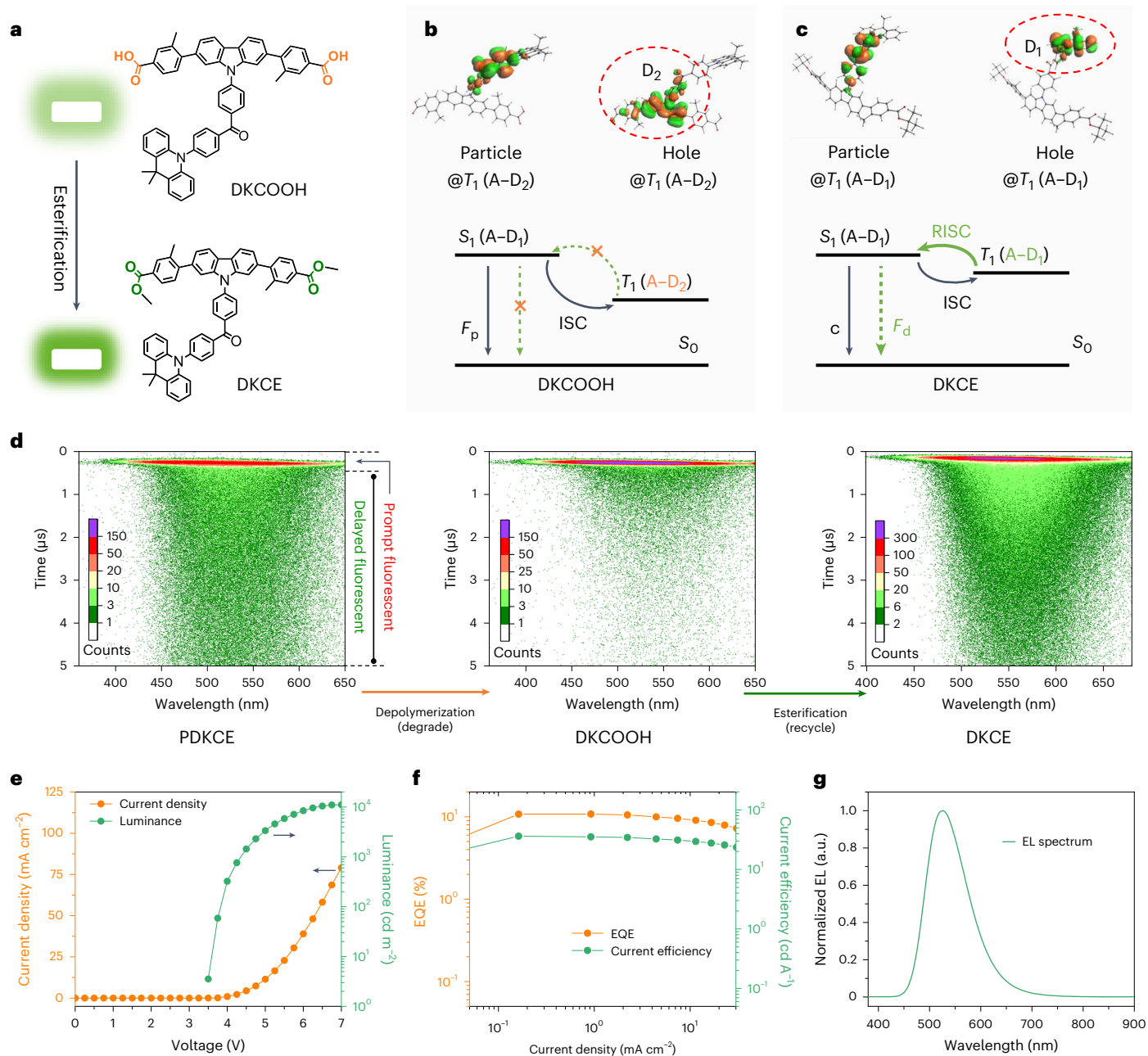
Fig. 4 | The recyclability of the TADF moiety in PDKCE. a, Recycling of the TADF moiety from its thermal-depolymerized product DKCOOH to DKCE by esterification. **b,c**, Hole/particle distributions at T_1 state of DKCOOH (**b**) and DKCE (**c**), and the schematics of their energy levels. A–D_1 and A–D_2, respectively, represent the charge transfer states from benzophenone–acridine and benzophenone–carbazole A–D pairs. **d**, Streak camera images in the time range of 0–5 μs at room temperature of PDKCE and the depolymerized product

DKCOOH (after heating), as well as the reesterification product DKCE. The thermal depolymerization condition is heating at 210 °C for 1 h in N_2 atmosphere. **e–g**, Device performance of OLED based on recycled DKCE. Representative current density–luminance–voltage traces (**e**), EQE–current density trace and current efficiency–current density trace (**f**) and EL spectrum of the OLED with recycled DKCE as EML (**g**). OLED structure: ITO/PEDOT:PSS (60 nm)/DKCE (40 nm)/TPBI (55 nm)/ LiF (1 nm)/aluminium.

purity without requiring any purification (Fig. 3d and Supplementary Fig. 15). In contrast, no depolymerization behaviour can be observed for PDKCM in the monitored temperature range (25–370 °C, Fig. 3b). It is worth noting that depolymerization of PDKCE occurred in both N_2 and air atmospheres (Supplementary Fig. 16a–c). However, we could not observe decarboxylation behaviour for PDKCE at higher temperatures, as reported in a previous study[24] (Supplementary Fig. 16d,e).

After depolymerization, PDKCE displays a slight red shift with minimal intensity change in the UV–vis spectrum and negligible change in the PL emission spectrum, indicating that the TADF core remained intact during the depolymerization process (Supplementary

Fig. 17). However, the PLQY decreased substantially from 60.9% to 2.8% with depolymerization, accompanied with a nearly vanished delayed fluorescent emission (Supplementary Figs. 18 and 19). In comparison, under these stressors, PDKCM shows negligible property changes reflected in various characterizations, including TGA, UV–vis, PL spectrum, PLQY and transient PL decay (Fig. 3b and Supplementary Figs. 17–19). Employing the distinct behaviours of PDKCE and PDKCM under thermal stress, we demonstrated a 'hidden' code with PDKCM serving as the code and PDKCE serving as the 'disguise'. Under thermal stress, the fluorescence emitted by the 'disguise' with depolymerizable PDKCE gradually diminishes, unveiling the 'hidden' code based
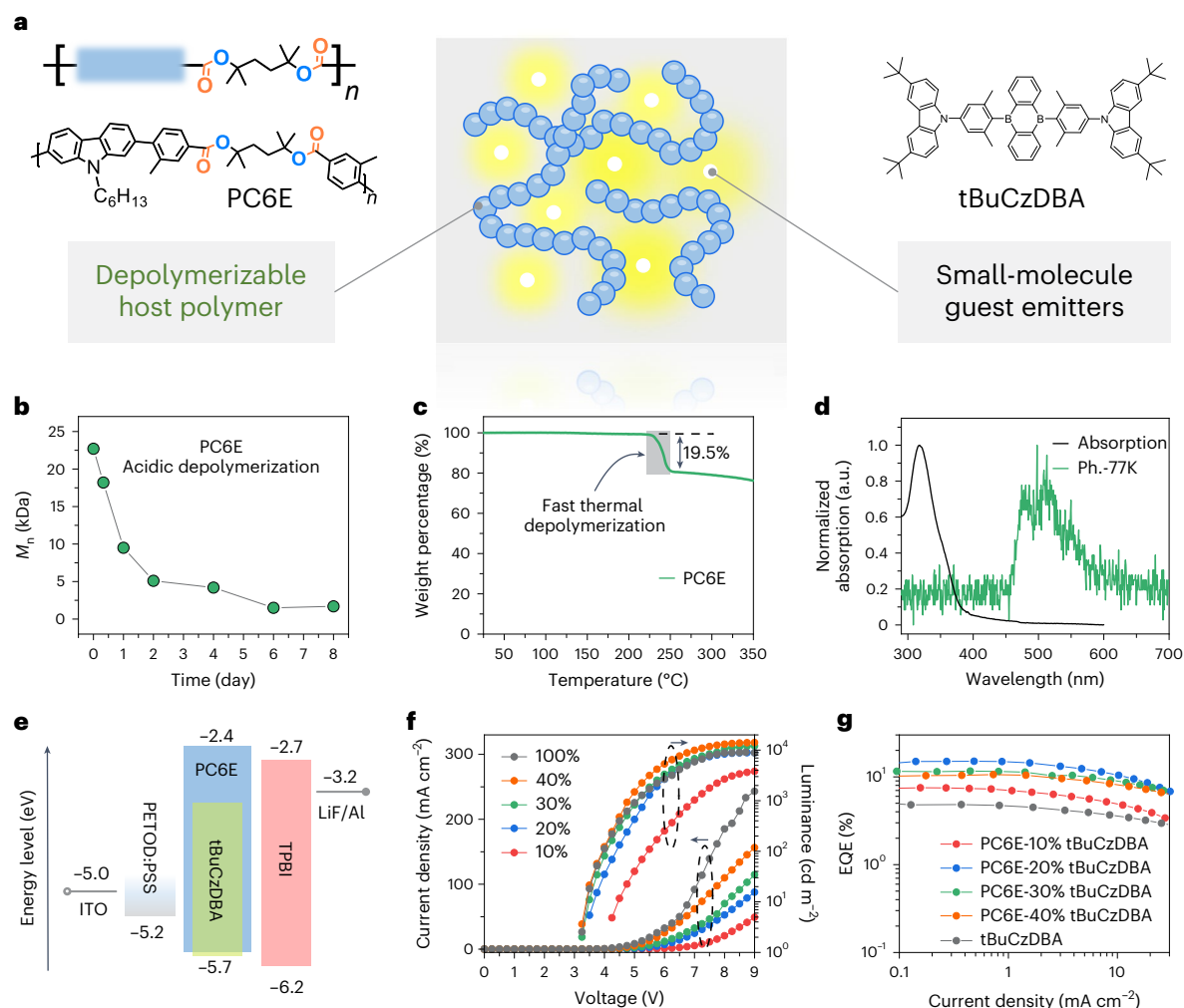
Fig. 5 | Depolymerizable host polymer PC6E. a, Schematic of EML composed of host/guest system, and the chemical structure of depolymerizable host polymer PC6E and the guest molecule tBuCzDBA used in this work. tBuCzDBA, 9,10-bis(4-(3,6-di-*tert*-butyl-9H-carbazol-9-yl)-2,6-dimethylphenyl)-9,10-diboraanthracene. **b**, The number average molar mass (M_n) of PC6E monitored over time in the mixed THF/HCl solution. **c**, The TGA curve of PC6E in N_2 atmosphere with a heating rate of 15 °C min^{-1}. **d**, Absorption spectrum of the PC6E film and low-temperature (77 K) phosphorescence spectrum of PC6E in 2-methyltetrahydrofuran solution. **e**, Schematic of energy levels for each material used in the OLED for the characterization of the EL performance of PC6E. **f,g**, Representative current density–luminance–voltage traces (**f**) and current density–EQE traces (**g**) for the OLEDs with PC6E/x wt.% tBuCzDBA as EML with different blending concentrations of 10, 20, 30, 40 and 100%.

on the non-depolymerizable PDKCM (Supplementary Fig. 20 and Supplementary Video 1).

To gain insights into the quenching of emission during depolymerization, we conducted comprehensive investigations, revealing that the generation of carboxylic acid groups results in a larger ΔE_{ST}, ultimately leading to the deactivation of TADF due to inefficiency of the RISC process (Supplementary Note 1 and Supplementary Figs. 21–23). Interestingly, the efficient TADF with a PLQY of 56.8% and a EQE of 10.8% can be restored by esterifying the carboxylic acid groups (Fig. 4a–g). This intriguing finding suggests that the depolymerized monomers hold promise for recycling in subsequent life applications, thereby demonstrating the viability of our design in promoting a circular economy.

Depolymerizable host polymer

In the realm of polymer-type emitters, a frequently employed strategy involves host–guest design to elevate luminescent performance. This mechanism hinges on the host polymer's ability to effectively mitigate concentration-induced quenching of TADF guest small molecules, primarily stemming from long-lived triplet excitons[32,33]. In this case, the same design concept is applied to the host polymer by combining TB-ester moieties with carbazole units in the polymer backbone, which is named as PC6E (Fig. 5a and Supplementary Figs. 1 and 3). The carbazole units provide the transport of charges and facilitate the formation of the excitons. Similar to PDKCE, PC6E demonstrates comparable depolymerization properties under both acidic and thermal stressors, as confirmed by GPC-tracking of the molar mass and TGA-tracking of the sample weight, respectively (Fig. 5b,c and Supplementary Figs. 12, 15, 16, 20 and 24).

To characterize the host performance of PC6E in the host–guest type emitters, we first studied its photophysical properties. The UV–vis spectrum is indeed dictated by the localized excited state of carbazole groups (Fig. 5d). It is crucial for the host materials to have a higher T_1 state (lowest triplet energy state) than the guest TADF emitters to confine the excitons in the guest emitter. T_1 was estimated by the onset of the low-temperature (77 K) phosphorescence, which is 2.71 eV. This value is high enough for most of TADF emitters (Fig. 5d). In particular, we selected the previously reported guest emitter tBuCzDBA[34] to blend with the host polymer PC6E, which has well-matched T_1 energy levels (Fig. 5d). Their good co-solubility in chlorobenzene enables smooth solution processing into homogeneous thin films. For this

emissive host–guest system we varied the doping ratio between 10 and 40 wt.% and tested the EL performance using the same device structure as above (Fig. 5e–g and Supplementary Fig. 25). First, compared with the tBuCzDBA guest-only emitters, all these host–guest emitters give higher EQEs (and also higher PLQY shown in Supplementary Fig. 26), which proves the suppression of the exciton quenching from the host–guest design. With the increase of the doping ratio from 10 to 40 wt.%, the current density and luminance gradually increase at the same voltage. This could come from the lower LUMO level of the guest material as compared with the host, which facilitates direct electron injection to the guest (Fig. 5e and Supplementary Fig. 6b) and increases charge-carrier mobility (Supplementary Fig. 27). A higher EQE of 15.1% (Fig. 5g) has been achieved with this host–guest design for degradable polymer-type emitters. Furthermore, the novel depolymerizable host PC6E exhibits comparable EL performance as the control non-depolymerizable host PC6D (Supplementary Fig. 28), providing further evidence that our depolymerizable/recyclable design, which incorporates TB-ester bonds into the polymer, has minimal influence on the TADF properties. It is worth noting that PC6E is not a suitable host for PDKCE or DKCE owing to its insufficiently high triplet state. (Supplementary Figs. 29 and 30).

Discussion

In this study, we have successfully developed sustainable TADF polymers with depolymerizability and recyclability by incorporating the TB-ester bond as a cleavable moiety in the polymer backbone, without compromising their high light-emitting properties. The resulting polymers exhibit solution processability, excellent luminescent performance, controllable depolymerizability and recyclability, positioning them as promising candidates for sustainable photonic technologies. Moreover, we have demonstrated the generalizability of our polymer design strategy, anticipating that optimizing the TADF core structures could yield higher efficiency and stability. This design strategy opens up new sustainable possibilities for the application of luminescent materials in diverse fields, such as biodegradable biomedical sensing, imaging and therapy, as well as optical computing and information storage.

Methods

Materials

The compounds (4-bromophenyl)(4-fluorophenyl)methanone and 2,7-dibromo-9H-carbazole were purchased from Combi-Blocks INC. The compound 9,9-dimethyl-9,10-dihydroacridine was purchased from Oakwood Products INC. The compounds 2,2′,2′-(1,3,5-benzinetriyl)-tris(1-phenyl-1-H-benzimidazole) (TPBI), 1,3,5-tris(3-pyridyl-3-phenyl) benzene (TmPyPB) and lithium fluoride (LiF) were purchased from Xi'an Polymer Light Technology Corp. Poly(3,4-ethylenedioxythiophene) polystyrene sulfonate (PEDOT:PSS) solution (CLEVIOS P VP CH 8000, 2.4–3.0 wt.% in water) was purchased from Heraeus Deutschland GmbH and Co. KG and used without changing concentration. Patterned indium tin oxide (ITO) glass substrate was purchased from Ossila Limited. Other general reagents and solvents were purchased from Sigma-Aldrich or Fisher Scientific. tBuCzDBA was purchased from Luminescence Technology Corp. PDKCM (M_n = 49.6 kDa, Đ = 2.2) is synthesized according to the reported procedures[4].

Synthesis

The depolymerizable and recyclable polymers were synthesized on the basis of a general Suzuki polycondensation procedure. The synthesis details can be found in Supplementary Information.

Simulation

All quantum chemical calculations were executed using the Gaussian 16 software. The molecular geometries were optimized in the ground state using the PBE0 functional with the 6-31G(d) basis set in the gas phase. TDDFT was applied to compute the lowest excited singlet and triplet states simulations, utilizing the optimized structures at the same level. For bond dissociation energy calculations, the same method as described in ref. 31 was used. The simplified molecular-input line-entry system (SMILES) string of the repeating unit of PDKCE molecule was used to create the SMILES strings for radicals by iteratively breaking all single, non-ring bonds in the parent molecule. The resulting list of SMILES strings was canonicalized and de-duplicated using the open-source cheminformatics RDKit (http://www.rdkit.org). All the open and closed shell structures were initially relaxed for geometry optimization using B3LYP-D3/6-31G(d). Unrestricted Kohn–Sham DFT calculations of radicals were then performed with the M06-2X functional and def2-TZVP basis set with the default ultra-fine grid for all numerical integrations. M06-2X/def2-TZVP was previously found to have a favourable trade-off between experimental accuracy and computational efficiency.

General characterization

NMR spectroscopy was performed on Bruker Ascend 9.4 T/400 MHz spectrometer or Bruker Ultra Shield 500 MHz NMR spectrometer. High-resolution MS with positive electrospray ionization mode was performed on Thermo Fisher orbitrap classic mass spectrometer.

Number average molar mass (M_n), mass average molar mass (M_w) and dispersity ($Đ = M_w/M_n$) were evaluated with Agilent HT-GPC system (SEC system 1) employing the Agilent PLgel 5 µm Mix-D separation column, Wyatt DAWN HELEOS II multi-angle light-scattering detector for absolute measurement of polymer molar mass and tetrahydrofuran (THF) as liquid phase at a temperature of 40 °C.

Absorption was measured using a Shimadzu UV-3600 Plus UV–Vis–NIR spectrophotometer. The film thicknesses were measured with Multiwavelength Laser Ellipsometers LSE-WS.

The PL spectra were measured in air under 300 nm excitation with a Horiba Spectrofluorometer-Fluorolog 3. Time-resolved emission experiments were performed on samples loaded in a liquid nitrogen-cooled cryostat, under vacuum. Time-resolved emission measurements were performed by exciting the sample with ultraviolet light pulses prepared by directing the output of a 35 fs Ti:sapphire laser (310 nm) into an optical parametric amplifier, with emission monitored using a streak camera. The PL quantum yield (PLQY) and low-temperature FL/PH spectra were measured using a LSM Series High-Power LED (310 nm, Ocean Optics) as the light source and a fibre optic-linked integrating sphere (integrating sphere is not used for low-temperature FL/PH) coupled with a QE Pro spectrometer (Ocean Optics). The samples within the integrating sphere were placed on a homemade stage to achieve a proper alignment with the excitation light source. For the recording of low-temperature FL/PH spectra liquid nitrogen was employed for cooling. The film samples were spin-coated on quartz substrates, except for the time-resolved emission measurements on silicon wafer substrate, in the glovebox from the polymer solutions of 8 mg ml⁻¹ in chlorobenzene. For the PLQY measurements of the TADF polymers with benzoic acid, the TADF polymers and benzoic acid are co-dissolved in chlorobenzene with total concentration of 8 mg ml⁻¹ for the spin-coating. The spin-coating condition is 1,500 rpm for 30 s, which is followed by annealing at 100 °C for 15 min.

Cyclic voltammetry was performed on a Multi PalmSens4 electrochemical analyser using dimethylformamide with tetra-n-butylammonium hexafluorophosphate (Bu₄NPF₆, 0.1 M) as electrolyte, an Ag/AgCl as reference electrode, a Pt disk as working electrode and a scan rate of 50 mV s⁻¹.

QR code patterns were printed on glass substrates with an Optomec Aerosol Jet 5X system. The degradable green pattern was created using an ink of PDKCE with a concentration of 2 mg ml⁻¹, dissolved in a 9:1 mixture of chlorobenzene and N-methyl-2-pyrrolidone. The centre pattern was printed with the ink of PDKCE (2 mg ml⁻¹) for green, PC6E (5 mg ml⁻¹) for blue, and 1:1 of PC6E and TPA-AQ[4] (3 mg ml⁻¹) for

red, which were separately dissolved in a 9:1 mixture of chlorobenzene and N-methyl-2-pyrrolidone.

Depolymerization conditions

Acidic depolymerization: in a glass vial, the polymer samples were dissolved in THF (5 mg ml^{-1}) under ultrasonication. For every 1 ml polymer solution, 8 µl of aqueous HCl (35 wt.%) were added via pipette. The vial, equipped with a stir bar, was places on a stirring hotplate. After evenly mixing, the solution was heated to 50 °C for depolymerization. After a certain period, 100 µl solution was transferred to a vial that contains 1 ml THF. The diluted solution is filtered through a polyvinylidene difluoride syringe filter with 0.45 µm pore size to prepare SEC samples. Number average M_n, M_w and $Đ = M_w/M_n$ were evaluated with Agilent 1260 Infinity II HT-GPC system (SEC system 2) employing the Agilent PLgel 5 µm MIXED-C separation columns, 1260 Infinity II Refractive Index detector for absolute measurement of polymer molar mass, and THF as liquid phase at a temperature of 40 °C.

Thermal depolymerization: TGA was measured with a Mettler Toledo TGA/STGA851e. A polymer sample (ca. 3 mg) was placed in a weighed TGA sample pan. The sample pan was carefully transferred into the TGA system. A nitrogen flow 20 ml min^{-1} was applied. The system was switched on and heated at 15 °C min^{-1} to 210 °C, then kept at 210 °C for 60 min to allow the full depolymerization of the polymer.

For TGA-coupled gas chromatography (GC)–MS measurements, TGAs were performed in a TA TGA5500 instrument. A total of 0.8 mg PDKCE or 2.2 mg PC6E were placed in an aluminium (Al) crucible. Samples were measured under ultra-high-purity helium gas (100 ml min^{-1}). Temperature was increased at a rate of 20 °C min^{-1} and gases were transferred to the GC–MS instrumentation via a heated (280 °C) transfer line. An Agilent Technologies 7890A GC system equipped with a non-polar capillary column (Agilent J&B HP-5 packed with (5%-phenyl)-methylpolysiloxane) coupled with a 5975 mass-selective detector spectrometer was used for the analyses of the gases released from the samples. A gas injection was triggered every 0.7 min from the beginning of the heating cycle and 0.25 ml of gas was sampled from the gases released by the compound and carrier gas (helium). Detection limit is typically better than 100 fg but this value can be larger, and it highly depends on the ionization efficiency of the different molecules in the compound. Mass spectra were scanned in the range of 10–600 U. Performance of the thermobalance of the TA TGA5500 was verified by using a certified sample of calcium oxalate monohydrate (European Pharmacopoeia Reference Standard) up to 1,000 °C.

OLEDs fabrication and testing

The ITO-coated glasses were first cleaned with 1 vol.% Hellmanex solution, isopropyl alcohol and de-ionized water, and then dried and further treated with O_2 plasma (150 W, 10 min). PEDOT:PSS dispersion was spin-coated on ITO substrates at 4,500 rpm for 1 min as a hole injection/hole transporting layer, followed by annealing at 150 °C for 30 min. Then, the emitting layers (EMLs) were spin-coated in the glovebox (with the levels of O_2 and H_2O below 0.5 ppm) from the polymer solutions of 8 mg ml^{-1} in chlorobenzene. The spin-coating condition is 1,500 rpm for 30 s, which is followed by annealing at 100 °C for 15 min. Next, thermal evaporations were carried out to sequentially deposit TPBI as the electron-transporting layer, LiF as the electron injection layer and Al as the cathode, with the corresponding deposition rates of 1, 0.1 and 10 Å s^{-1}, respectively. The current density–voltage–luminance (J–V–L) measurements were carried out with the freshly fabricated devices at room temperature in an N_2 filled glovebox. A Keithley 2450 source metre and a fibre optic integration sphere coupled with a QE Pro spectrometer (Ocean Optics) were used for the measurements. The OLED devices were tested on top of the integrating sphere window, where only forward light emission can be collected. The absolute OLED emission was calibrated versus a standard visible–near-infrared light source (HL-3P-INT-CAL plus, Ocean Optics).

Reporting summary

Further information on research design is available in the Nature Research Reporting Summary linked to this article.

Data availability

The data that support the findings of this study are available within this article and its Supplementary Information. Additional data are available from the corresponding authors upon request. Source data are provided with this paper.

References

1. Zhang, D., Huang, T. & Duan, L. Emerging self-emissive technologies for flexible displays. *Adv. Mater.* **32**, 1902391 (2019).
2. Fang, F. et al. Thermally activated delayed fluorescence material: an emerging class of metal-free luminophores for biomedical applications. *Adv. Sci.* **8**, e2102970 (2021).
3. Taal, A. J. et al. Optogenetic stimulation probes with single-neuron resolution based on organic LEDs monolithically integrated on CMOS. *Nat. Electron.* **6**, 669–679 (2023).
4. Liu, W. et al. High-efficiency stretchable light-emitting polymers from thermally activated delayed fluorescence. *Nat. Mater.* **22**, 737–745 (2023).
5. Zhang, Z. et al. High-brightness all-polymer stretchable LED with charge-trapping dilution. *Nature* **603**, 624–630 (2022).
6. MacLeod, M., Arp, H. P. H., Tekman, M. B. & Jahnke, A. The global threat from plastic pollution. *Science* **373**, 61–65 (2021).
7. Jehanno, C. et al. Critical advances and future opportunities in upcycling commodity polymers. *Nature* **603**, 803–814 (2022).
8. Yao, Y. et al. A robust vertical nanoscaffold for recyclable, paintable, and flexible light-emitting devices. *Sci. Adv.* **8**, eabn2225 (2022).
9. Gomez, E. F., Venkatraman, V., Grote, J. G. & Steckl, A. J. Exploring the potential of nucleic acid bases in organic light emitting diodes. *Adv. Mater.* **27**, 7552–7562 (2015).
10. Zhao, J. et al. Microplastic fragmentation by rotifers in aquatic ecosystems contributes to global nanoplastic pollution. *Nat. Nanotechnol.* **19**, 406–414 (2023).
11. Lei, T. et al. Biocompatible and totally disintegrable semiconducting polymer for ultrathin and ultralightweight transient electronics. *Proc. Natl Acad. Sci. USA* **114**, 5107–5112 (2017).
12. Tran, H. et al. Stretchable and fully degradable semiconductors for transient electronics. *ACS Cent. Sci.* **5**, 1884–1891 (2019).
13. Irimia-Vladu, M. Green' electronics: biodegradable and biocompatible materials and devices for sustainable future. *Chem. Soc. Rev.* **43**, 588–610 (2014).
14. Kong, D., Zhang, K., Tian, J., Yin, L. & Sheng, X. Biocompatible and biodegradable light-emitting materials and devices. *Adv. Mater. Technol.* **7**, 2100006 (2021).
15. Tian, S. et al. Complete degradation of a conjugated polymer into green upcycling products by sunlight in air. *J. Am. Chem. Soc.* **143**, 10054–10058 (2021).
16. Uva, A., Lin, A. & Tran, H. Biobased, degradable, and conjugated poly(azomethine)s. *J. Am. Chem. Soc.* **145**, 3606–3614 (2023).
17. Wang, W. Z. et al. Degradable conjugated polymers: synthesis and applications in enrichment of semiconducting single-walled carbon nanotubes. *Adv. Funct. Mater.* **21**, 1643–1651 (2011).
18. Chiong, J. A. et al. Impact of molecular design on degradation lifetimes of degradable imine-based semiconducting polymers. *J. Am. Chem. Soc.* **144**, 3717–3726 (2022).
19. Al-Attar, H. et al. Polylactide-perylene derivative for blue biodegradable organic light-emitting diodes. *Polym. Int.* **70**, 51–58 (2020).
20. Baldo, M. A. et al. Highly efficient phosphorescent emission from organic electroluminescent devices. *Nature* **395**, 151–154 (1998).

21. Uoyama, H., Goushi, K., Shizu, K., Nomura, H. & Adachi, C. Highly efficient organic light-emitting diodes from delayed fluorescence. *Nature* **492**, 234–238 (2012).

22. Hatakeyama, T. et al. Ultrapure blue thermally activated delayed fluorescence molecules: efficient HOMO-LUMO separation by the multiple resonance effect. *Adv. Mater.* **28**, 2777–2781 (2016).

23. Liu, J., Kadnikova, E. N., Liu, Y., McGehee, M. D. & Frechet, J. M. Polythiophene containing thermally removable solubilizing groups enhances the interface and the performance of polymer-titania hybrid solar cells. *J. Am. Chem. Soc.* **126**, 9486–9487 (2004).

24. Son, S. Y., Samson, S., Siddika, S., O'Connor, B. T. & You, W. Thermocleavage of partial side chains in polythiophenes offers appreciable photovoltaic efficiency and significant morphological stability. *Chem. Mater.* **33**, 4745–4756 (2021).

25. Dong, Q. et al. Depolymerization of plastics by means of electrified spatiotemporal heating. *Nature* **616**, 488–494 (2023).

26. Liu, W. et al. Novel strategy to develop exciplex emitters for high-performance OLEDs by employing thermally activated delayed fluorescence materials. *Adv. Funct. Mater.* **26**, 2002–2008 (2016).

27. Zhu, A. et al. Rational design of multi-functional thermally activated delayed fluorescence emitter for both sensor and OLED applications. *New J. Chem.* **46**, 10940–10950 (2022).

28. Boutry, C. M. et al. Biodegradable and flexible arterial-pulse sensor for the wireless monitoring of blood flow. *Nat. Biomed. Eng.* **3**, 47–57 (2019).

29. Reeder, J. T. et al. Soft, bioresorbable coolers for reversible conduction block of peripheral nerves. *Science* **377**, 109–115 (2022).

30. Zarei, M., Lee, G., Lee, S. G. & Cho, K. Advances in biodegradable electronic skin: material progress and recent applications in sensing, robotics, and human-machine interfaces. *Adv. Mater.* **35**, 2203193 (2023).

31. St. John, P. C. et al. Quantum chemical calculations for over 200,000 organic radical species and 40,000 associated closed-shell molecules. *Sci. Data* **7**, 244 (2020).

32. Hung, M. K., Tsai, K. W., Sharma, S., Wu, J. Y. & Chen, S. A. Acridan grafted poly(biphenyl germanium) with high triplet energy, low polarizability and external heavy-atom effect for highly efficient sky-blue TADF electroluminescence. *Angew. Chem. Int. Ed.* **58**, 11317–11323 (2019).

33. Shao, S. et al. Bipolar poly(arylene phosphine oxide) hosts with widely tunable triplet energy levels for high-efficiency blue, green, and red thermally activated delayed fluorescence polymer light-emitting diodes. *Macromolecules* **52**, 3394–3403 (2019).

34. Wu, T.-L. et al. Diboron compound-based organic light-emitting diodes with high efficiency and reduced efficiency roll-off. *Nat. Photonics* **12**, 235–240 (2018).

Acknowledgements

Author contributions

J.X. conceived the research. W.L., Y.W. and J.X. designed the experiments. A.V., C.Z. and H.C. performed the simulation. S.H. and Y.Z. helped with printing demonstrations. B.T.D. and R.D.S performed the PL transient decay measurement. C.Z. and G.W. carried out the PLQY measurement. D.C. and P.G. helped with the measurement of low-temperature FL/PH spectra. H.J. helped with initial exploratory experiments for degradable light-emitting polymer. J.M., S.W. and J.X. supervised the research. W.L., Y.W., J.M., S.W. and J.X. wrote the paper. All the authors contributed to the discussion and paper revision.

Competing interests

J.X., Y.W. and W.L. are inventors on a pending patent filed by the Argonne National Laboratory (IN-23-027). All other authors declare no competing interests.

Additional information

Supplementary information The online version contains supplementary material available at https://doi.org/10.1038/s41893-024-01373-z.

Correspondence and requests for materials should be addressed to Jianguo Mei, Sihong Wang or Jie Xu.

Peer review information *Nature Sustainability* thanks Xiaohong Zhang and the other, anonymous, reviewer(s) for their contribution to the peer review of this work.

Reprints and permissions information is available at www.nature.com/reprints.

Publisher's note Springer Nature remains neutral with regard to jurisdictional claims in published maps and institutional affiliations.

nature portfolio

Corresponding author(s): Jie Xu, Sihong Wang, Jianguo Mei

Last updated by author(s): Apr 19, 2024

Reporting Summary

Nature Portfolio wishes to improve the reproducibility of the work that we publish. This form provides structure for consistency and transparency in reporting. For further information on Nature Portfolio policies, see our Editorial Policies and the Editorial Policy Checklist.

Statistics

For all statistical analyses, confirm that the following items are present in the figure legend, table legend, main text, or Methods section.

n/a	Confirmed	
☒	☐	The exact sample size (*n*) for each experimental group/condition, given as a discrete number and unit of measurement
☒	☐	A statement on whether measurements were taken from distinct samples or whether the same sample was measured repeatedly
☒	☐	The statistical test(s) used AND whether they are one- or two-sided *Only common tests should be described solely by name; describe more complex techniques in the Methods section.*
☒	☐	A description of all covariates tested
☒	☐	A description of any assumptions or corrections, such as tests of normality and adjustment for multiple comparisons
☒	☐	A full description of the statistical parameters including central tendency (e.g. means) or other basic estimates (e.g. regression coefficient) AND variation (e.g. standard deviation) or associated estimates of uncertainty (e.g. confidence intervals)
☒	☐	For null hypothesis testing, the test statistic (e.g. *F*, *t*, *r*) with confidence intervals, effect sizes, degrees of freedom and *P* value noted *Give P values as exact values whenever suitable.*
☒	☐	For Bayesian analysis, information on the choice of priors and Markov chain Monte Carlo settings
☒	☐	For hierarchical and complex designs, identification of the appropriate level for tests and full reporting of outcomes
☒	☐	Estimates of effect sizes (e.g. Cohen's *d*, Pearson's *r*), indicating how they were calculated

Our web collection on statistics for biologists contains articles on many of the points above.

Software and code

Policy information about availability of computer code

Data collection	n/a for computer code.
Data analysis	n/a for computer code.

For manuscripts utilizing custom algorithms or software that are central to the research but not yet described in published literature, software must be made available to editors and reviewers. We strongly encourage code deposition in a community repository (e.g. GitHub). See the Nature Portfolio guidelines for submitting code & software for further information.

Data

Policy information about availability of data

All manuscripts must include a data availability statement. This statement should provide the following information, where applicable:
- Accession codes, unique identifiers, or web links for publicly available datasets
- A description of any restrictions on data availability
- For clinical datasets or third party data, please ensure that the statement adheres to our policy

We have provided a full data availability statement in the manuscript.

Human research participants

Policy information about studies involving human research participants and Sex and Gender in Research.

Reporting on sex and gender	n/a
Population characteristics	n/a
Recruitment	n/a
Ethics oversight	n/a

Note that full information on the approval of the study protocol must also be provided in the manuscript.

Field-specific reporting

Please select the one below that is the best fit for your research. If you are not sure, read the appropriate sections before making your selection.

☐ Life sciences   ☐ Behavioural & social sciences   ☒ Ecological, evolutionary & environmental sciences

For a reference copy of the document with all sections, see nature.com/documents/nr-reporting-summary-flat.pdf

Ecological, evolutionary & environmental sciences study design

All studies must disclose on these points even when the disclosure is negative.

Study description	n/a
Research sample	n/a
Sampling strategy	n/a
Data collection	n/a
Timing and spatial scale	n/a
Data exclusions	n/a
Reproducibility	n/a
Randomization	n/a
Blinding	n/a

Did the study involve field work?   ☐ Yes   ☒ No

Reporting for specific materials, systems and methods

We require information from authors about some types of materials, experimental systems and methods used in many studies. Here, indicate whether each material, system or method listed is relevant to your study. If you are not sure if a list item applies to your research, read the appropriate section before selecting a response.

Materials & experimental systems

n/a	Involved in the study
☒	Antibodies
☒	Eukaryotic cell lines
☒	Palaeontology and archaeology
☒	Animals and other organisms
☒	Clinical data
☒	Dual use research of concern

Methods

n/a	Involved in the study
☒	ChIP-seq
☒	Flow cytometry
☒	MRI-based neuroimaging